



## An Empirical and Numerical Approach to Evaluate Submarine Resistance in Fully Submerged Configuration with Experimental validation

Muhammad Asad<sup>1</sup>, Asif Mansoor<sup>1</sup>, Behzad Ahmed Zai<sup>1</sup>, Murtaza Hussain<sup>1</sup>, Najam us Saqib<sup>2,\*</sup>

### ARTICLE INFO

#### Article history:

Received 14 Mar 2023;  
in revised from 14 Mar 2023;  
accepted 02 Apr 2023.

#### Keywords:

RANSE, Computation Fluid Dynamics (CFD), Submarine, Drag, Multi-phase flow.

### ABSTRACT

Submarine technology is an undisputed cornerstone for coastal defenses round the globe. Not only it enables a naval force to operate with covertness, but also bestows a nuclear power with second-strike capabilities. Aforementioned features have engendered an enhanced focus towards the research and development in different aspects of submarine technology. One of the main areas of research in submarine design is the identification of optimum ship performance design parameters. Forgoing in view, the analysis of hydrodynamic aspects plays a vital role in resistance and efficiency of the propulsion system, which holds prime significance. Given the fact that designing of submarine is incomplete without the optimum resistance, the present research work focuses on different methods to calculate the resistance. In this paper, the resistance of submarine (DARPA SUBOFF) is computed in submerged condition using RANSE based CFD model with k-e realizable function and cut cell technique. The estimated CFD results are validated with the experimental results provided by DARPA. The accuracy observed for the applied technique is up to 97%. Same validated technique is applied on the arbitrary submarine to calculate the submerged resistance. Along with CFD, different empirical techniques that are only applicable to submerged bodies are also studied for analytical calculation of resistance with experimental validation. The most efficient empirical technique is identified with respect to the submerged geometries. This research will be helpful for the resistance prediction of other marine vehicles, particularly for powering prediction of submarine.

© SEECMAR | All rights reserved

### 1. Introduction.

During the designing of a ship or a submarine, the analysis of hydrodynamic aspects is one of the most crucial steps to get an optimum ship's performance. The analysis serves as a tool to find the resistance and efficiency of the propulsion system. The resistance of the ship is basically dependent on the shape of the hull and the wetted surface. It is also affected by variations in the operating conditions of the ship including speed, trim, and draught. From the resistance, the required engine power of the vessel can be calculated.

There are several different methods used for calculating the ship resistance as shown in **Fig. 1**. There are experimental and numerical methods which are used for analyzing the flow field around underwater vehicles. During experimental analysis, model testing is a vital part for the resistance prediction of ship as the flow is always complex around the hull and cannot be accurately predicted without practical experimentation. The results obtained from towing tank or experimental analysis are considered to be the most accurate compared to all other resistance prediction techniques, but the method is costly as well as time consuming.

The other method to calculate resistance is the empirical method. In empirical method, both "traditional and standard series analysis method" and "regression-based method" are used. The method is more of a theoretical approach than practical but there is a natural limitation on the accuracy of the approach

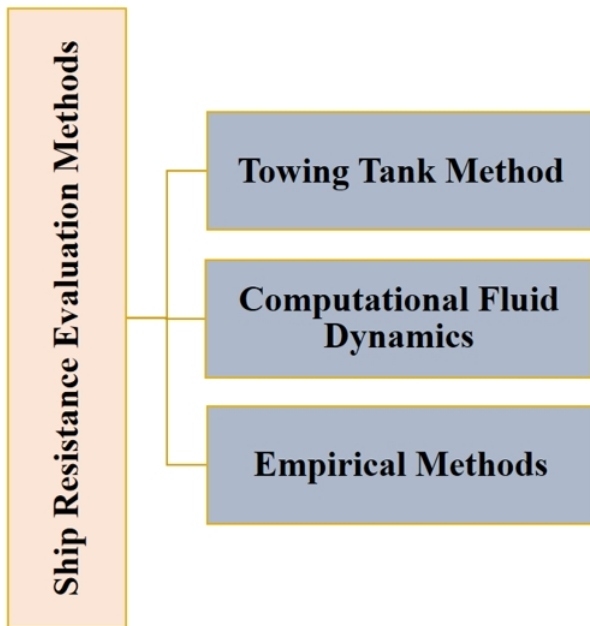
<sup>1</sup>Department of Engineering Sciences, PN Engineering College, National University of Sciences and Technology (NUST), Karachi, Pakistan.

<sup>2</sup>Department of Mechanical Engineering, NED University, Karachi, Pakistan.

\*Corresponding author: Najam us Saqib. E-mail Address: najamus-saqib1987@gmail.com.

i.e. the method computes resistance without using more complex hull definition parameters. Instead of towing tank or empirical methods, CFD is now commonly used for calculating and simulating the ship resistance. DNS, LES, and RANS are the methods which are commonly used in CFD. The marine problems usually utilize the RANS model since the other two methods are computationally expensive. Given the fact that designing of submarine is incomplete without the optimum resistance, the present research work focuses on empirical and CFD analysis to calculate the resistance. In the past, Grooves et al.[1] Documented the complete geometrical details of DRAPA Suboff which provides a base for the validation of CFD results. Later on Huang [2] documented the experimental measurements of the flow fields from an axi-symmetrical body with and without appendages that were made in the Carderock Division Naval Surface Warfare Center (CDNSWC) and TracorHydrodynamics Ship Model Basin (HSMB). The experimental data served as the data base for the Computational Fluid Dynamics (CFD) validations and other submarine related flow field analyses.

Figure 1: Ship resistance evaluation methods.



Source: Authors.

In a research published by Phillips et al.[3]the resistance of AUV's is calculated using CFD analysis. According to the research the power requirement and range of vehicle is dependent on the hull resistance just like submarines. Later on, RANSE based CFD analysis is carried out by Sukas et al. [4] for calculating the total resistance of ships and submarine.

The CFD analysis is carried out by Moonesun et al.[5]on bare hull forms and investigated different ways to reduce resistance. The CFD analysis is also carried out on tourists' submarines by Yaseer M. Ahmed [6] for analyzing the flow around the submarine. In the research,RANSE scheme has been used whereas for the numerical simulations, the Omega Reynold tur-

bulent model is adapted. Later on, the empirical work on submarine resistance is conducted by M. Moonesun et al. In their research, they presented different experimental formulas for calculating bare hull resistance in submerged condition. Different methods for calculating the drag were also compared. From their findings, it was concluded that experimental method is best for calculating resistance, but in case of its unavailability, other methods are also viable if the errors are estimated correctly[7].The research conducted by Ahadyanti et al. [8]on mini-submarine also described the analysis of submerged resistance of mini-submarines using both empirical and CFD techniques.

The experimental and numerical study of a submarine and propeller behaviors in submerged/surface conditions is conducted by A. Vali et al. [9]. They observed that, while performing powering analysis of submarines, hull/propeller interaction has great significance. Optimizing the shape of the submarine is one of the major tasks in marine engineering across the globe, as prescribed by Aditya et al. [10]in their research. The research also discusses the outline for optimum design of submarines. The researches in the past by Kinnas and Hsin [11] , Ohkusu [12], Gao and Davies [13], and Ghassemi[14] figured out the potential flow method for computing CFD simulation. Later on, research conducted by Turnock& Wright [15] reveal that finite volume method is more credible as compared to the potential flow method. The research conducted by Gohil et al. [16]shows that the SST  $k-\omega(2)$  equation) model is the most suitable method for simulating the flow field around submarines and propellers. The research conducted by Rhee et al. [17]outlined the VOF method for even spilling breaking waves and bubbly free surface. The research further elaborates on several multiphase flow problems related to surface piercing hydrofoils. In this paper, the resistance is evaluated on different models in submerged condition using analytical and numerical techniques, later validated using experimental data. This approach is equally applicable to other marine structures related to powering prediction of submarines.

## 2. Mathematical Formulation.

In this study, RANSE equations with  $k-\epsilon$  and  $k-\omega$  SST models are used for single and multi-phase respectively. This method is named after Osborne Reynolds, the person who first described this method[18]. RANS equation for the unsteady, three dimensional and incompressible flows are basically the continuity equation and can be given as Eq. (1). Whereas the momentum equation can be represented as Eq. (2)

$$\frac{\partial U_i}{\partial x_i} = 0 \quad (1)$$

$$\frac{\partial U_i}{\partial t} + \frac{\partial(U_i U_j)}{\partial x_j} = \frac{-1}{\rho} \frac{\partial p}{\partial x_i} + \frac{\partial}{\partial x_j} \left[ \vartheta \left( \frac{\partial U_i}{\partial x_j} + \frac{\partial U_j}{\partial x_i} \right) \right] - \frac{\partial \overline{u_i u_j}}{\partial x_j} \quad (2)$$

Since the steady state condition is considered for the analysis so the first term of Eq. (2) is cancelled and is not considered

for the simulation. Here, mean flow velocity vector is defined by  $U_i$ , kinematic viscosity by  $\nu$  and density by  $\rho$ . Now,

$$\frac{\partial U_i}{\partial x_j} + \frac{\partial U_j}{\partial x_i} = 2S_{ij} \quad (3)$$

Here, the term  $S_{ij}$  represents the mean strain tensor. The term  $-\overline{u_i u_j}$  in Eq. (2) represents the Reynold stress tensor and can be represented by  $\tau_{ij}$ . Eq. (2) can now transform into the given form

$$\frac{\partial(U_i U_j)}{\partial x_j} = \frac{-1}{\rho} \frac{\partial p}{\partial x_i} + \frac{\partial}{\partial x_j} 2\nu S_{ij} - \frac{\partial \tau_{ij}}{\partial x_j} \quad (4)$$

$$\frac{\partial(U_i U_j)}{\partial x_j} = \frac{-1}{\rho} \frac{\partial p}{\partial x_i} + \frac{\partial}{\partial x_j} (2\nu S_{ij} + \tau_{ij}) \quad (5)$$

The term  $\tau_{ij}$  consist of turbulence eddy viscosity  $\mu_t$ . The Boussinesq hypothesis is used to connect this model to RANS equation using following relation

$$\tau_{ij} = -\mu_t S \quad (6)$$

$$\mu_t = \frac{-1}{2} \frac{\rho \tau_{ij}}{S_{ij}} \quad (7)$$

According to RANSE equation the turbulence eddy viscosity is computed from

$$\mu_t = C_\mu \rho \frac{k^2}{\epsilon} \quad (8)$$

The value of  $k$  and  $\epsilon$  are calculated from the turbulence equation and is given below

$$\rho \frac{\partial k}{\partial t} + \rho \bar{\mu}_j \frac{\partial k}{\partial x_j} = \tau_{ij} \frac{\partial \bar{u}_i}{\partial x_j} - \rho \epsilon + \frac{\partial}{\partial x_j} \left[ \left( \mu + \frac{\mu_T}{\sigma_1 \epsilon} \right) \frac{\partial k}{\partial x_j} \right] \quad (9)$$

$$\rho \frac{\partial \epsilon}{\partial t} + \rho \bar{\mu}_j \frac{\partial \epsilon}{\partial x_j} = \alpha^3 \frac{\epsilon}{k} \tau_{ij} \frac{\partial \bar{u}_i}{\partial x_j} - \beta^3 \rho \frac{\epsilon^2}{k} + \frac{\partial}{\partial x_j} \left[ \left( \mu + \frac{\mu_T}{\sigma_2 \epsilon} \right) \frac{\partial \epsilon}{\partial x_j} \right] \quad (10)$$

The obtained parameters are put into Eq. (9) to determine the turbulence eddy viscosity with the help of Eq.(5), Reynold-stress tensor is obtained, the term that form the core of RANS equations.

### 3. Computational Domain of 3D Hull.

3-D modeling is required to calculate the resistance of submarines. Two different geometries are used in this research. The first one is DARPA's model and second model is designed similar to DARPA's model but with different parameters as shown in **Fig. 2(a)** and **Fig. 2(b)**. Both models with scale ratio 1:1 is employed in CFD to estimate resistance of submarines at different variations of speed. The simplified version of physical domain considering the imposition of boundary conditions and object's geometrical representation is called computational domain as shown in **Fig. 2(c)** and **Fig. 2(d)**. All the important physical characteristics must be retained by this domain, but

Table 1: Computational Domain of both Models.

Parameter	Domain Standard	Model 1	Model 2
Length upstream (m)	2*C	8.712	12.000
Length downstream (m)	4*C	17.424	24.000
Depth (m)	2*C	8.712	12.000
Breadth (m)	1.25*C	5.445	7.500

Source: Authors.

insignificant features can be neglected. The computational domain used for single-phase analysis is according to the standard as mentioned by Lieu et al. [4] and shown in **Table 1**.

Where C is the model length. Since the body is axially symmetrical, only half of the hull form is considered in the problem to reduce the time of analysis.

### 4. Meshing.

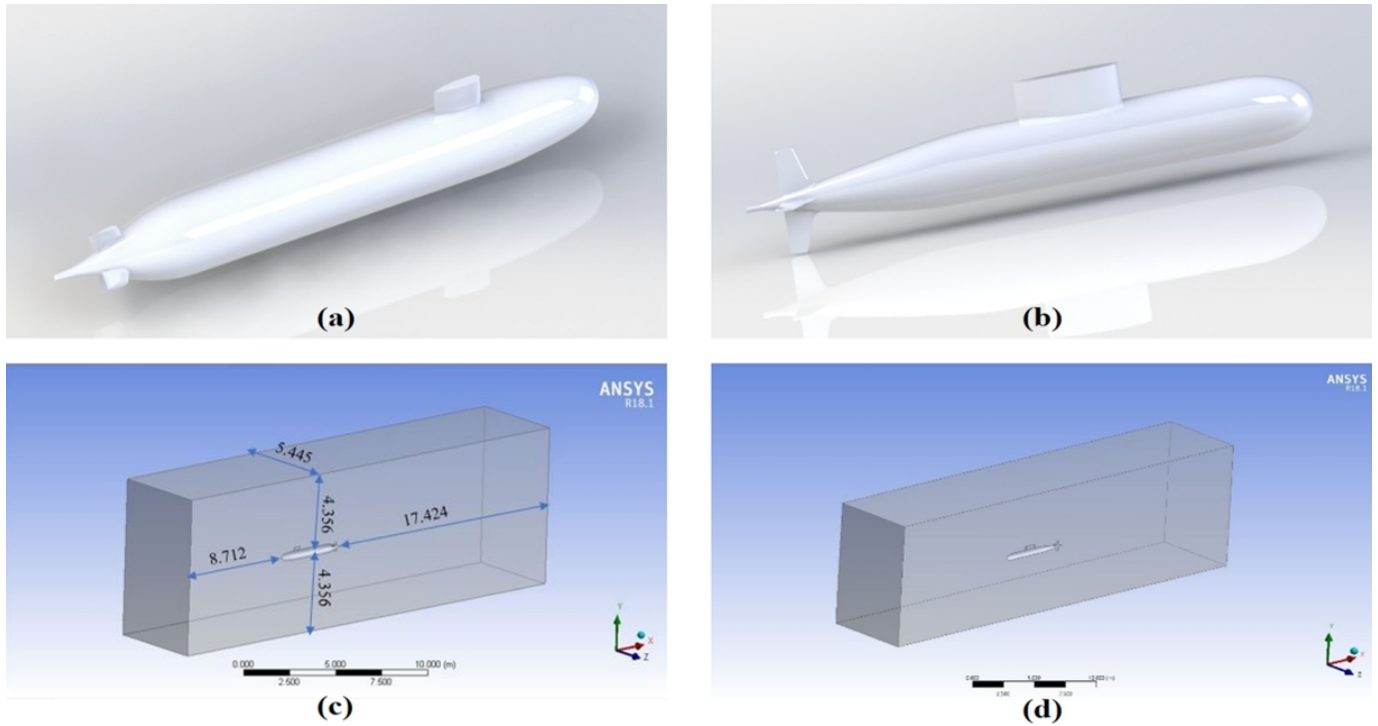
In single-phase analysis, meshing is done by using Cartesian grid methods commonly known as cut-cell methods or embedded boundary methods. In the cut-cell method, uniform Cartesian grid is used over most of the domain while for bodies that are intersected by the boundary, Cartesian cells cut into a small irregular cell. The technique is effective since it allows automated mesh generation process around complex 3-D bodies. Also, it permits the use of standard-high resolution shock capturing methods away from the boundary which is difficult to develop on unstructured grids. Body sizing, face sizing, and edge meshing were performed to refine the mesh. Mesh independence study means that the results obtained from a mesh show only the physical characteristics of the flow field and is not affected by numerical abnormalities. Mesh independence study is always required before proceeding to CFD simulations. Five different meshes are created to obtain stable solution with sufficient number of elements. The number of meshes ranges from 70918 cells for the coarse mesh to 3941858 cells for the dense mesh. Mesh independence is depicted in **Fig. 3**. Based on the simulations conducted at max speed i.e. (17.79 knots) of the given model, the results observed are shown in **Table 2**. Based on the study, it was decided to use the mesh of 881399 cells for drag calculation. It captures the flow behavior adequately, while saving the computational resources.

Table 2: Results of Mesh Independence Study.

No of Elements	Drag Coefficient	Drag (N)
70918	0.031134	872.0
486382	0.028810	806.9
881399	0.0289406	810.5
3941844	0.0289441	810.6
3941858	0.0289513	810.8

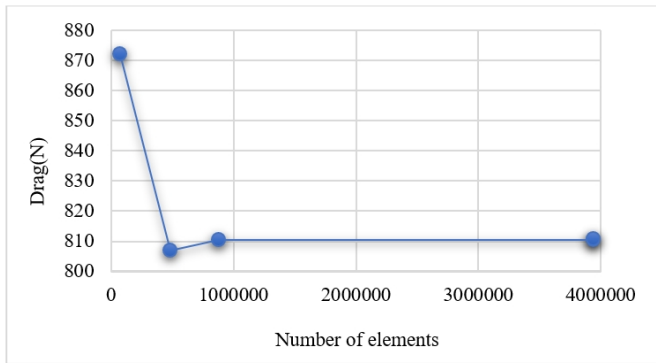
Source: Authors.

Figure 2: Computational Domain.



Source: Authors.

Figure 3: Mesh independence study.



Source: Authors.

Meshing is finalized on the bases of the grid independence test and the detailed properties of mesh used for calculating the drag of submarine are given below. The details of meshing for Model 1 are tabulated in **Table 3**. All remaining functions are set as default in ANSYS meshing module. After applying all these size functions on geometry, the final mesh is obtained as shown in **Fig. 4**.

### 5. CFD Setup and Boundary Conditions.

k-epsilon realizable model is used in single phase analysis while Water-liquid is used as material in single phase. Coupled scheme is used in both single and multi-phase analysis. coupled

Table 3: Meshing details of Model 1.

Sizing	Element Size		Size function	Growth rate
	Model 1	Model 2		
Body sizing	0.2	0.2	Proximity and curvature	1.20
Face sizing	0.009	0.001	Proximity and curvature	1.20
Edge sizing	0.009	0.001	Curvature	1.20

Source: Authors.

approach will provide an effective, robust, and efficient solution which forms the basis for single-phase implementation for these steady fluids. In comparison to other segregated solution schemes, the performance of this scheme is much better and effective[19] second order scheme is applied in pressure mode for single phase. The method is highly recommended when the flows are compressible and are not of porous nature, fan, or multiphase flows. The boundary conditions are given in **Table 4**.

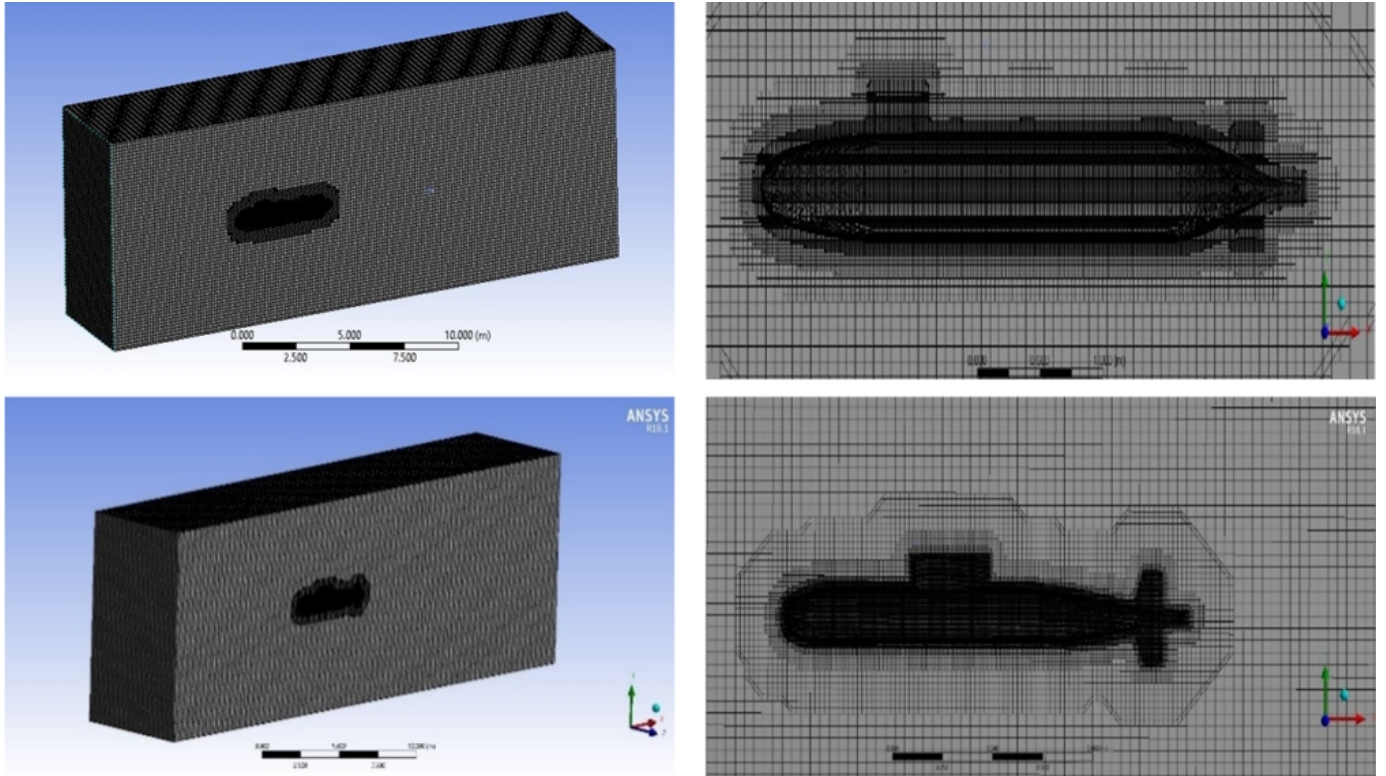
### 6. Empirical Methods for Resistance Calculations.

There are four different methods for calculating the resistance of submarine in fully submerged conditions which are stated as under.

#### 6.1. Method 1.

The total resistance ( $C_{TS}$ ) of the submarine for bare hull can be estimated by the following expression. This method cal-

Figure 4: Final mesh of provided models.



Source: Authors.

Table 4: The details of boundary conditions.

Parameter	Boundary condition
Inlet	Velocity inlet
Outlet	Pressure outlet
Wall	symmetry
Top	No slip/ Stationary wall
Bottom	No slip/ Stationary wall
Symmetry	Symmetry

Source: Authors.

calculates the bare hull resistance by several diagrams as demonstrated in reference [20].

$$C_{TS} = C_{FS} + C_R + C_A$$

Where,

$C_{FS}$  = Coefficient of frictional resistance

$C_R$  = Coefficient of residuary resistance

$C_A$  = Correlation allowance for model to full scale

$C_{RM}$  is assumed to be independent of Reynold's number and the value of the coefficient can be determined from model resistance experiment. According to this assumption:

$$C_{RM} = C_{RS}$$

The error in the assumption is compensated by the correlation allowance.  $C_A$  is determined ultimately from first class trials of the new submarine, but during the initial stage (design & model stage) the value can be assumed from the data of previous class submarines. A typical value of this coefficient is in the range of 0.004 to 0.006. The value of  $C_R$  and  $C_A$  is taken as 0.0007 and 0.0004 respectively, as given in [7].

$C_{FS}$  for the submarine can be calculated by using ITTC empirical formulas given below:

$$C_{FS} = \frac{0.075}{(\log_{10} R_N - 2)^2}$$

The total resistance of the ship can then be calculated by the following relation:

$$R_{TS} = C_{TS} * \frac{1}{2} * \rho * S * V^2$$

Where,

$\rho$  = Density of seawater

S = Wetted surface area of hull

V = Velocity of the vehicle

### 6.2. Method 2.

This method is mentioned in the practical ship hydrodynamics book [21] and was adopted by Moonesun et al. in their research [7]. Prior to applying this method, there are some conditions which must be satisfied, these conditions are given as follows:

- Length to diameter ratio must be in the given range i.e.  $5 \leq \frac{L}{D} \leq 7$
- Depth of submergence must be 5 times or greater than that of the diameter i.e.  $ak$

After satisfying the above-mentioned conditions, the hull resistance of a submarine can be calculated by using the following equation.

$$R_T = \frac{1}{2} C_T \rho A V^2$$

Where,

$A$  = Wetted surface area of bare hull and appendage resistance must be added to obtain total resistance.

$C_T$  = The total resistance coefficient and can be calculated as.

$$C_T = C_F + C_{VP}$$

$C_{VP}$  = Pressure resistance coefficient that is given below.

$$C_{VP} = C_{form} = k C_0$$

Where,

$k$  = Form coefficient and the value of  $k$  can be obtained using the following relation between length and diameter of the submarine.

$$k = \frac{D}{L} + 1.5 \left(\frac{D}{L}\right)^3$$

$C_{fo}$  can be calculated by ITTC formula as calculated in method 1, which is given below:

$$C_{fo} = \frac{0.075}{(\log_{10} Re - 2)^2}$$

$C_F$  = Frictional resistance coefficient that can be calculated using the given relation:

$$C_F = C_{fo} + \delta C_F$$

$$\delta C_F = 0.05 C_F$$

Where,

The value of  $\delta C_F$  is taken as 0.0001.

### 6.3. Method 3.

This alternative method to calculate the bare hull resistance is mentioned in reference [7] Like previous methods, the total resistance of the hull can be calculated by the same formula which is given below:

$$R_T = \frac{1}{2} C_T \rho A V^2$$

Where

$C_T$  = Total friction resistance coefficient and can be calculated using the following relation:

$$C_T = C_F \left[ 1 + 1.5 \left(\frac{D}{L}\right)^{1.5} + 7 \left(\frac{D}{L}\right)^3 \right]$$

The frictional resistance coefficient ( $C_F$ ) can be calculated by the formula:

$$C_F = C_{F0} + \delta C_F$$

$C_{F0}$  is then calculated by the ITTC formula (as mentioned in previous methods) while the value for  $\delta C_F$  is taken as 0.0001 as given in the research [7].

### 6.4. Method 4.

This method is quite like method 3, except that the way to calculate the total friction resistance coefficient is different. The formula for calculating the total friction resistance is given below. The remaining parameters are calculated in a similar way as in method 3.

$$C_T = C_F \left[ 3 \left(\frac{D}{L}\right) + 4.5 \left(\frac{D}{L}\right)^{0.5} + 21 \left(\frac{D}{L}\right)^3 \right]$$

## 7. Results and Discussion.

### 7.1. CFD Results.

The validation has been made for DARPA Suboff. The analysis is performed on all six velocities and the results obtained from CFD are shown in **Table 5**.

Table 5: CFD results.

V(m/sec)	Drag Coefficient	CFD Results (N)	Exp Results (N)	% error
3.0506	0.0037056	103.785	102.3	1.4
5.1444	0.0098344	275.438	283.8	2.9
6.0961	0.0135100	378.434	389.2	2.8
7.1610	0.0182678	511.638	526.6	2.8
8.2311	0.0237180	664.328	675.6	1.6
9.1519	0.0289406	810.556	821.1	1.2

Source: Authors.

It is clearly observed from the results that the error in the CFD results is less than 3% for all velocities which shows that the technique used for finding out the resistance is perfect and can be trustfully applied to find the drag of other submarines. The validated CFD technique is applied on model 2 to calculate the unknown resistance of an arbitrary submarine having similar type of hull but different length. the results obtained from CFD are shown in **Table 6**. The pressure and velocity contour for both models at velocity 3.0506 m/sec are shown in **Fig. 5**.

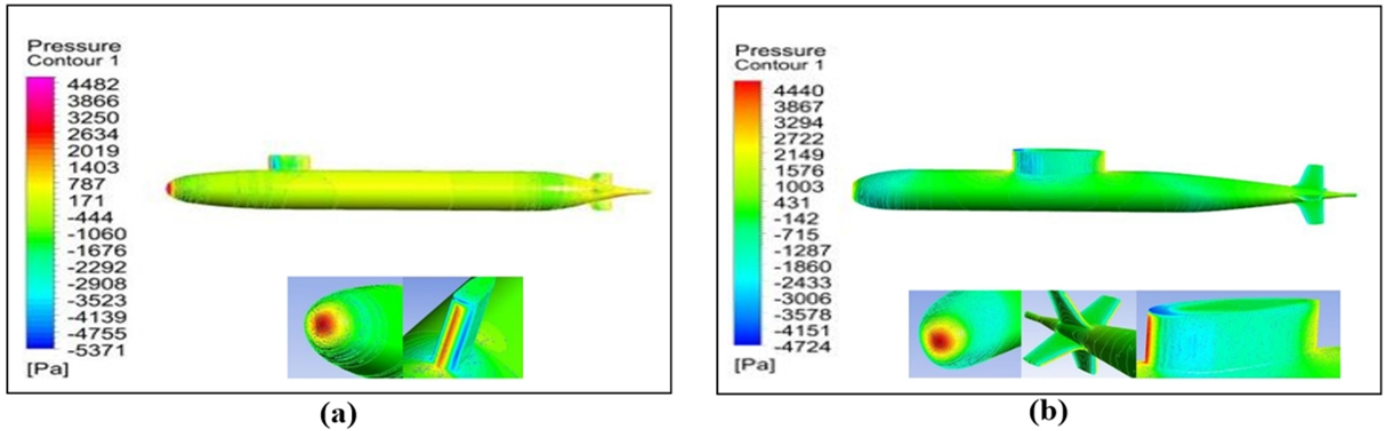
Table 6: CFD results of drag parameters.

V (m/sec)	Drag Coefficient	Drag (N)
3.0506	0.0102000	284.720
5.1444	0.0051412	776.218
6.0961	0.0071239	1075.54
7.1610	0.0097096	1465.90
8.2311	0.0126979	1916.92
9.1519	0.0155764	2351.64

Source: Authors.

It can be seen from the pressure contours that there are two stagnation points on the submarine i.e. on the bow and stern. The pressure is maximum on these stagnation points. From the stagnation point at bow, the flow is accelerated around the

Figure 5: (a) Pressure contour for Model 1 at velocity 3.0506 m/sec, (b) Pressure contour for Model 2 at velocity 3.0506 m/sec.



Source: Authors.

bridge of the hull where the pressure increases. Along the parallel middle body, the boundary layer grows, the flow is then accelerated as it reaches the stern taper, where the boundary layer is growing rapidly and becoming thicker as shown in Fig. 6.

It can be observed from the different views of velocity contours that the velocity is minimum or close to zero at stagnation points. The velocity is increased as the flow passed through stagnation points. The velocity again decreased drastically near the bridge. The boundary layer grows in the parallel middle body and the flow is accelerated until it reaches the stern part. Large vortex structures form behind the stern which forms the wake region.

### 7.2. Empirical Results.

The obtained results from these methods are given below in the tabulated form for naked and appendage hull resistance at six different velocities. Normally, appendage resistance contributes to 35% of the total resistance according to research [7], but their individual appendage resistance also includes appendages of bridge fin, stern and bow planes, upper and lower rudder and the resistance due to sonar fairing and keel. Since our model geometry did not contain bow planes and sonar, we have added only 23% appendage resistance in bare hull and have excluded the percentage of the appendages which were not included in our geometry. **Table 7** shows the resistance results calculated using model 1. All the empirical methods (which we have studied earlier) are again applied on model 2 to calculate the resistance. The obtained results from these methods at six different velocities are given below in the tabulated form in **Table 8**, refer to the detailed calculations of model 2.

The detailed comparison of different empirical techniques, CFD, and experimental results are shown in **Table 9**. The resistance percentages are included in methods 1, 2, and 3 for comparison since CFD results are for the appended hull. All values in the table are in N. The graphical representation of the different methods are shown in **Fig. 7**.

Table 7: Resistance results calculated using model 1.

V(m/sec)	Method 1		Method 3		Method 4	
	$R_{T(woa)}(N)$	$R_{T(wa)}(N)$	$R_{T(woa)}(N)$	$R_{T(wa)}(N)$	$R_{T(woa)}(N)$	$R_{T(wa)}(N)$
3.051	170	209	134	164	229	282
5.144	454	558	350	430	600	738
6.096	626	770	479	589	822	1011
7.161	849	1044	645	793	1107	1361
8.231	1105	1360	834	1026	1431	1760
9.152	1350	1660	1015	1249	1742	2143

Source: Authors.

Table 8: Resistance results calculated using model 2.

V(m/sec)	Method 1		Method 3		Method 4	
	$R_{T(woa)}(N)$	$R_{T(wa)}(N)$	$R_{T(woa)}(N)$	$R_{T(wa)}(N)$	$R_{T(woa)}(N)$	$R_{T(wa)}(N)$
3.051	111	137	89	110	161	198
5.144	298	366	234	288	420	517
6.096	410	505	320	394	575	707
7.161	556	684	432	531	774	952
8.231	723	890	558	687	1001	1231
9.152	884	1088	679	835	1217	1497

Source: Authors.

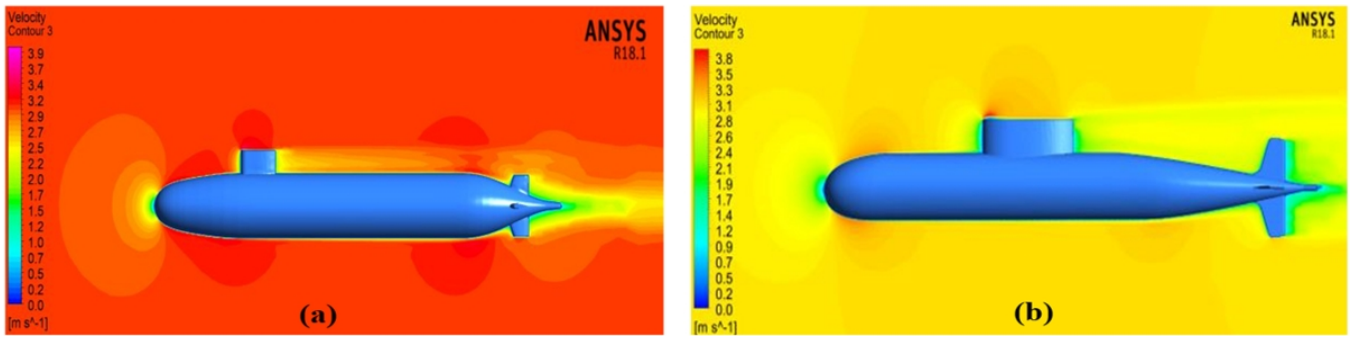
Table 9: Comparison of Different Resistance Prediction Techniques.

V(m/sec)	Exp Results	Method 1	Method 3	Method 4	CFD
3.051	102.3	137.370	110.530	198.140	103.785
5.144	283.8	366.770	288.770	517.630	275.438
6.096	389.2	505.090	394.730	707.630	378.434
7.161	526.6	684.540	531.520	952.730	511.638
8.231	675.6	890.470	687.310	1231.900	664.328
9.152	821.1	1088.240	835.860	1497.120	810.556

Source: Authors.

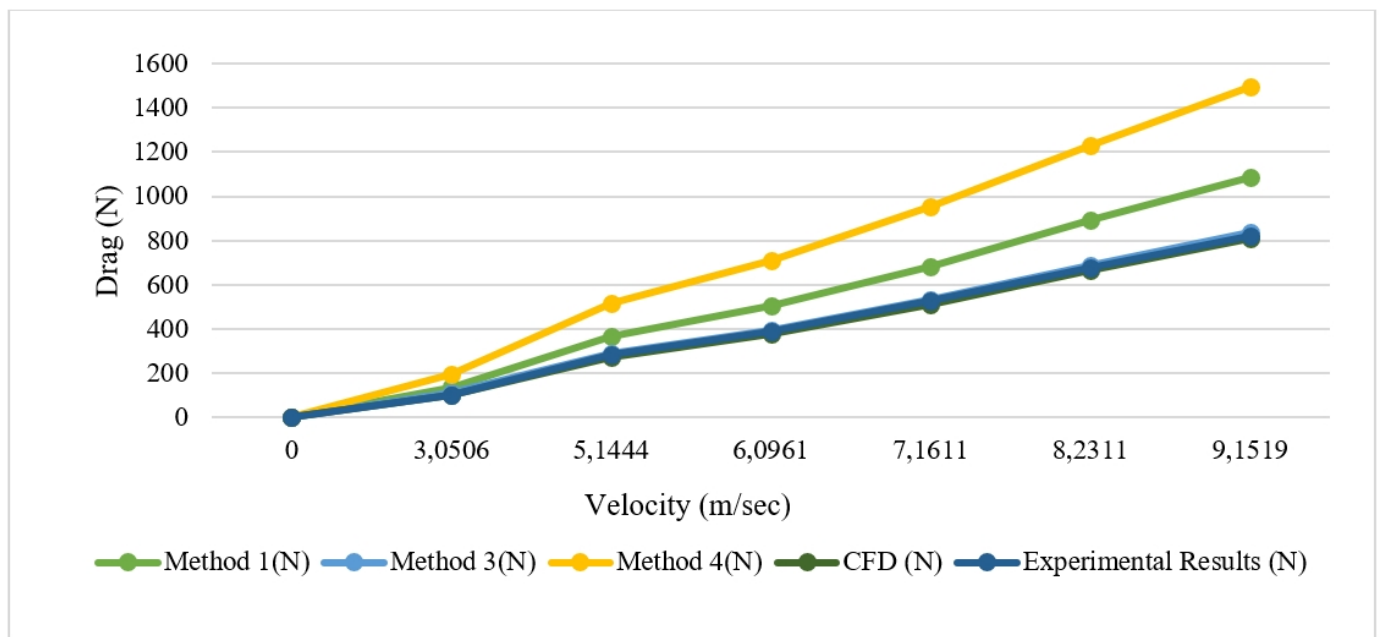
The graphical and tabulated results with percentages error shows that the values obtained from CFD results are very closed to actual results. The error percentages are less than 3% so among all other methods, CFD is the most authentic method for finding the resistance. Among empirical methods, the results of method 3 are closed to experimental results with less than 2% error except for the first velocity having an error percentage of 8% but since the method is empirical it is not authentic till it

Figure 6: (a) Velocity contour for Model 1, (b) Velocity contour for Model 2, at velocity 3.0506 m/sec.



Source: Authors.

Figure 7: Comparison graph of different methods for Model 1.



Source: Authors.

applied to different submarine. Method 1 is not very close to experimental results and having an error of 34%. Method 4 is too diverged from the experimental results. All these methods will again be applied to second submerged bodies for finalizing the methods of resistance prediction. The detailed comparison of different empirical techniques and CFD results of drag for model 2 are shown in **Table 10**. The same theme of presentation is used as was used in the case of model 1. The comparison of different Techniques in graphical form is given in **Fig. 8**.

The graphical and tabulated results with percentage error show that the comparison with CFD reveals the fact that method 4 is very close to the experimental results. The error in the method is less than 9%. The results of method 3 have slightly diverged from CFD results with an error of about 30%. The results obtained from method 3 are totally diverged with an error of about 47%. Although method 1 gives error greater than method 3 in the first case and method 4 in the second case but the method 1 is more consistent as it gives around the same er-

Table 10: Comparison Of Empirical Results with CFD for Model 2.

V(m/sec)	Exp Results	Method 1	Method 3	Method 4	CFD
3.051	102.3	137.370	110.530	198.140	103.785
5.144	283.8	366.770	288.770	517.630	275.438
6.096	389.2	505.090	394.730	707.630	378.434
7.161	526.6	684.540	531.520	952.730	511.638
8.231	675.6	890.470	687.310	1231.900	664.328
9.152	821.1	1088.240	835.860	1497.120	810.556

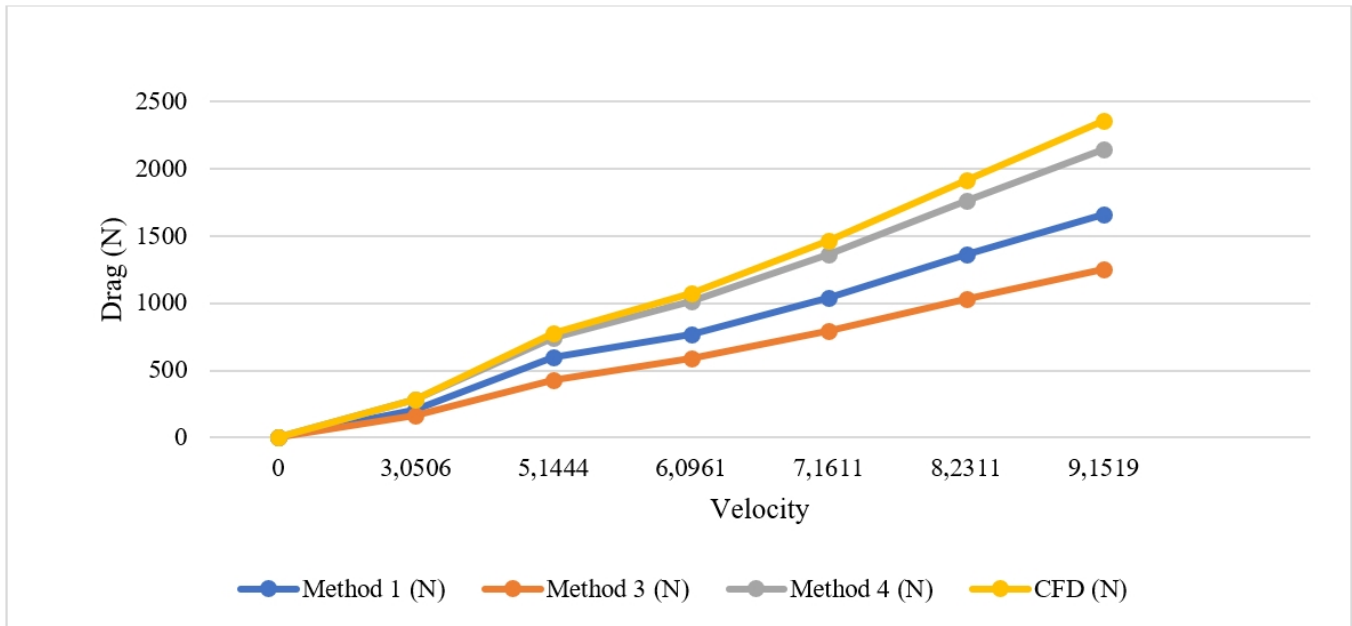
Source: Authors.

ror in both cases so a rough approximation can be made with method 1 for finding the resistance of submarine.

**Conclusions.**

Drag of submarines and ship is evaluated using CFD analysis on submerged and surfaced conditions. The DARPA Suboff

Figure 8: Comparison graph of different methods for Model 2.



Source: Authors.

model which is basically a research submarine is used for verification and validation purposes. Two other geometries, besides DARPA SUBOFF are also used in the research for both single and multi-phase analysis. Along with CFD method, the resistance values of submerged bodies are also evaluated using different empirical approaches at six different velocities. Cut cell method is applied for meshing in the submerged case as the technique is the most effective for automated mesh generation around 3-D complex bodies and allows the use of standard high-resolution shock capturing methods away from the boundaries.

K-epsilon realizable function is used for finding the drag of submerged bodies. The verification and validation exercise on the submerged resistance case, shows that the applied technique is most effective for drag calculations since the error percentages with respect to experimental results are less than 3% on all six velocities. Different empirical techniques are applied and Method 1 is selected as authentic empirical method for rough or approximate resistance prediction of submarine. This research will be very helpful for resistance prediction of submarine.

## References.

- [1] Ming S Chang. Thomas T Huang. Nancy C. Groves, "Geometric Characteristics Of DARPA Suboff Models (DTRC MODEL No. 5470 and 5471)," DARPA, March, 1989. W364W9791.
- [2] Han-Lieh Lieu. Thomas T Huang, "Summary Of Darpa Suboff Experimental Program," June 1998. W364W9791.
- [3] Alexander Phillips . Maaten Furlong . Stephen R Turnock , "The Use Of Computational Fluid Dynamics To Assess The Hull Resistance Of Concept Autonomous Underwater Vehicle," July 2007. W364W9791.

- [4] Omer Faruk Sukas . Omer Kemal Kinaci . Sakir Bai, "Computation Of Total Resistance Of Ship and a Submarine By A Rans Based CFD," October 2014. W364W9791.

- [5] Mohammad Moonesun . Yuri Mikhailovich . Hosein Dalayeli, "CFD analysis on the Bare Hull Form Of submarines For Minimizing The Resistance," International Journal Of Maritime Technology, vol. Vol 3, Winter 2015. W364W9791.

- [6] Y. M. Ahmed, "Viscous Resistance Prediction Of Tourist Submaarine At Various Speeds," International Review Of Mechanical Engineering , July 2016. W364W9791.

- [7] Mohammad Moonesun . Mehran Javadi . Pejman Charmdooz . Karol Uri Mikhailovich, "Evaluation Of Submarine Model Test In Towing Tank and Comapariosn with CFD And Experimental Formulas For Fully Submerged Resistance," Indina Journal Of Geo Marine Sciences, vol. 42 (8), December 2013. W364W9791.

- [8] Gita Marina Ahadyanti . Wasis Dwi Aryawan . Muhammad Fyan Dinggi, "Submerged Resistance Analysis Of Mini Submarine Using Computational Fluid Dynamics," in Senta (Marine Technology For Sustainable Technology ), 2017. W364W9791.

- [9] A Vali .B Saranjan .R Kamali, "Experimental And Numerical Study Of A Submarine And Propeller Behaviour In Submerged And Surfaced Condition," Journal Of Applied Fluid Mechanics, vol. 11, 2018. W364W9791.

- [10] Aditya Chivate . Saurabh Khuje . Shubham Vinchurkar . Anjuit Dafle, "Design And Optimization Of An Underwater Vehicle Vessel For Speed Augmentation Using CFD," International Journal Of Mechanical And Production Engineering , vol. 6, 2018. W364W9791.

- [11] Kinnas . C Y Hsin , "Boundary Element Method For The Analysis Of The Unsteady Flow Around Extreme Propeller

Geometry,” AIAA Journal, vol. 32 (8), pp. 688-696, 1992. W364W9791.

[12] Ohkusu, ”Advances In Marine Hydrodynamics, Computational Mechanics,” 1996. W364W9791.

[13] Gao. X W. T G Davies , ”Boundary Element Programming In Mechanics,” in Cambride University Press, New York, 2002. W364W9791.

[14] Ghassemi H, ”Hydrodynamics Characteristics Of Marine Propeller In Steady And Unsteady Wake Flows,” Journal Of Science And Technology Of AmirKabir, vol. 14(54), pp. 81-98, 2003. W364W9791.

[15] Turnock. S R . A M Wright, ”Directly Coupled Fluid Structural Model Of A Ship Rudder Behind A Propeller,” in Marine Structures , 2000, pp. 53-72.W364W9791.

[16] Gohil . P.P. R.P Saini, ”Numerical Study Of Cavitation In Francis Turbine Of A Small Hydro Power Plant,” Journal

Of Applied Fluid Mechanics, vol. 9(1), pp. 357-365, 2016. W364W9791.

[17] Rhee SH .Makarov BP .Krishinan H et al., ”Assessment Of The Volume Of Fluid Method For Free surface Wave Flow,” Journal Of Marine Science Technology, vol. 10(4), pp. 173-180, 2005. W364W9791.

[18] O, Reynolds, ”On The Dynamical Theory Of Incompressible Viscous Fluids And The Determination Of The Criterion,” vol. Philosophical Transactions Of The Royal Society Of London (A), pp. 123-164, 1895. W364W9791.

[19] Ansys Fluent 12.0 Usser Guide.W364W9791.

[20] Roy Burcher & Louis Rydill, Concepts In Submarine Design. W364W9791.

[21] Volker Bertram, Practical Ship Hydrodynamics. W364W9791.